JACS
JOURNAL OF THE AMERICAN CHEMICAL SOCIETY
Article
pubs.acs.org/JACS

Mechanistic Characterization of (Xantphos)Ni(I)-Mediated Alkyl Bromide Activation: Oxidative Addition, Electron Transfer, or Halogen-Atom Abstraction

Justin B. Diccianni, Joseph Katigbak, Chunhua Hu, and Tianning Diao*

Department of Chemistry, New York University, 100 Washington Square East, New York, New York 10003, United States

Supporting Information

Ni(I)-mediated single-electron oxidative activation of alkyl halides has been extensively proposed as a key step in Ni-catalyzed cross-coupling reactions to generate radical intermediates. There are four mechanisms through which this step could take place: oxidative addition, outer-sphere electron transfer, inner-sphere electron transfer, and concerted halogen-atom abstraction. Despite considerable computational studies, there is no experimental study to evaluate all four pathways for Ni(I)-mediated alkyl radical formation. Herein, we report the isolation of a series of (Xantphos)Ni(I)−Ar complexes that selectively activate alkyl halides over aryl halides to eject radicals and form Ni(II) complexes. This observation allows the application of kinetic studies on the steric, electronic, and solvent effects, in combination with DFT calculations, to systematically assess the four possible pathways. Our data reveal that (Xantphos)Ni(I)-mediated alkyl halide activation proceeds via a concerted halogen-atom abstraction mechanism. This result corroborates with previous DFT studies on (terpy)Ni(I)- and (py)Ni(I)-mediated alkyl radical formation, and contrasts with the outer-sphere electron transfer pathway observed for $(PPh_3)_4Ni(0)$-mediated aryl halide activation. This case study provides insight into the overall mechanism of Ni-catalyzed cross-coupling reactions and offer a basis for differentiating electrophiles in cross-electrophile coupling reactions.

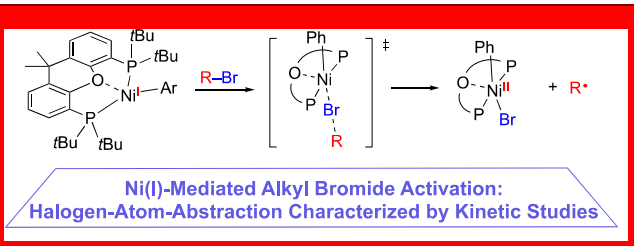

INTRODUCTION

Recent advances in Ni-catalyzed cross-coupling reactions have found important synthetic applications.[1] Historical[2] and contemporary[3] mechanistic studies provide evidence for single-electron transfer pathways in the presence of Ni(I) and Ni(III) intermediates.[4] In the catalytic cycles of Ni-catalyzed cross-coupling and cross-electrophile coupling reactions, alkyl halides are proposed to be activated by Ni(I)−halide or Ni(I)−carbyl intermediates via single-electron oxidative activation to form radicals (Scheme 1).[3] Capture of the radical by a Ni(II) intermediate gives rise to a Ni(III) species, which undergoes reductive elimination to generate the product. The single-electron oxidative activation step and the formation of radical intermediates with Ni(I) catalysts has created opportunities for stereoconvergent coupling of alkyl halides,[1h,5] and the combination of Ni catalysis with photoredox catalysis has given access to new reactivity.[6] In addition, electrophile activation is critical to the chemoselectivity and scope of cross-electrophile coupling reactions, when both aryl and alkyl halides are present and competing for activation.[1h] Therefore, it is crucial to understand the mechanistic details of single-electron oxidative activation of electrophiles mediated by Ni(I) complexes.

How are electrophiles activated by Ni(I) species and how are radicals generated? Several different pathways are possible for Ni(I)-mediated radical formation from aryl and alkyl halides (Scheme 2). Ni(I) complexes have been shown to undergo two-electron oxidative addition with MeI to form Ni(III),[7] from which a radical could be ejected to generate Ni(II) (*Pathway 1*).[8] Single electron transfer pathways, either outer-sphere (*Pathway 2*) or inner-sphere, via an encounter complex (*Pathway 3*), have been invoked in a number of mechanistic proposals,[2,3c] and proceed through electron transfer from Ni(I) to the alkyl/aryl halides to form radical anions, followed by subsequent homolytic C−X bond cleavage to eject a radical.[2,3] Many of these proposals are primarily based on the study of $Ni(0)(PEt_3)_4$-mediated aryl halide oxidative addition by Kochi and co-workers, who concluded that aryl radicals are formed via outer-sphere electron transfer as the rate-determining step.[9,10] A macrocyclic Ni(I) complex, relevant to cofactor F430 of methanogenic bacteria, has been proposed to activate alkyl halides via electron transfer.[11] Finally, recent DFT calculations on a number of Ni(0)[12] and Ni(I)[13] systems propose the concerted halogen-atom-abstraction pathway (*Pathway 4*). In particular, this pathway was found to be operational in (terpy)Ni−Me,[13a] (PNP)Ni-(CO),[13b] (pybox)NiMe,[13c] and (py)NiPh[3h] mediated alkyl halide activation. Although the halogen-atom-abstraction pathway prevails in recent DFT studies, there is limited experimental support. Moreover, despite the observation of stoichiometric radical formation with several well-defined Ni(I) complexes,[3e,14] there is no systematic experimental

Received: December 18, 2018
Published: January 6, 2019

DOI: 10.1021/jacs.8b13499
J. Am. Chem. Soc. XXXX, XXX, XXX−XXX

Scheme 1. Possible Mechanisms of Ni-Catalyzed Cross-Coupling with Ni(I)-Mediated Radical Formation as Key Steps

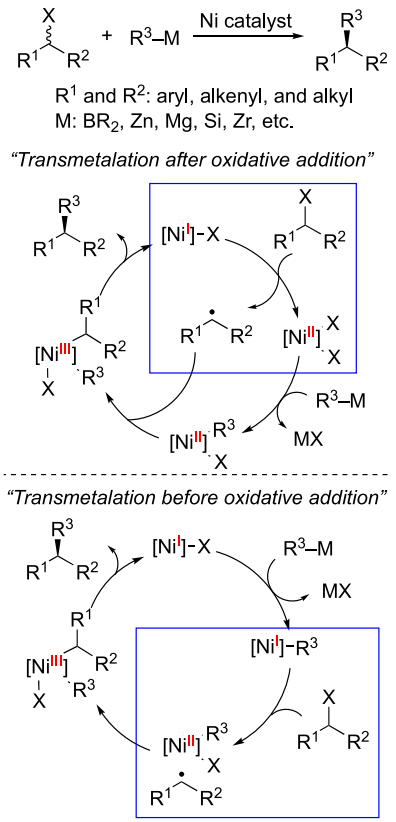

Scheme 2. Possible Pathways for Ni-Mediated Radical Formation from Alkyl Halides

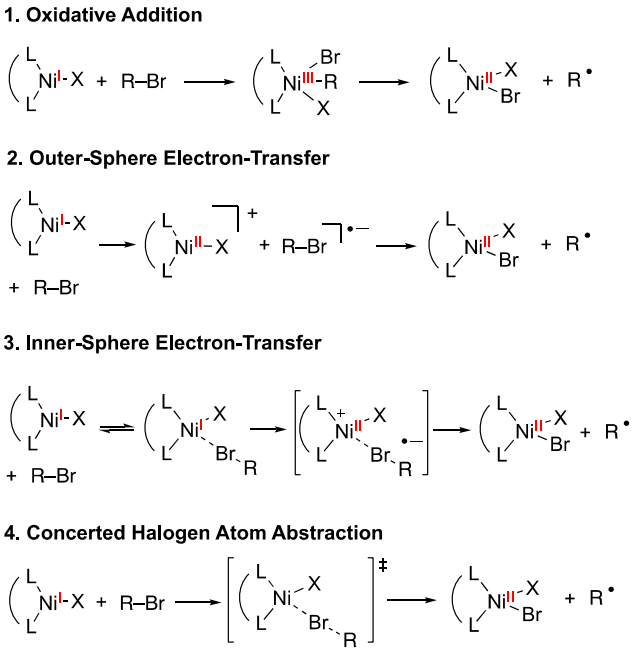

study to evaluate all four pathways for Ni(I)-mediated alkyl radical formation.

In light of the prevalent proposals of Ni(I)-mediated single-electron activation of electrophiles to form radicals in catalytic studies,[2,3] we herein, report the synthesis and isolation of (*t*Bu-Xantphos)Ni(I)−aryl complexes that enabled a detailed study on the mechanism of Ni(I)-mediated alkyl halide activation to form radicals. Although the vast majority of Ni-catalyzed cross-coupling reactions utilize nitrogen-based ligands, the catalytic reactivity of the Ni/Xantphos system shown here and the analogy of the transition states between (Xantphos)Ni−Ar and (terpy)NiMe[13a] suggest that this work could provide insight into the electrophile activation step in cross-electrophile coupling reactions.

RESULTS

Synthesis and Characterization of (*t*Bu-Xantphos)Ni(I) Complexes. The synthesis and isolation of well-defined Ni(I)−carbyl complexes is a significant synthetic challenge due to the radical, and often unstable, nature of Ni(I) complexes.[15] Previous examples use tridentate ligands to stabilize the Ni(I) oxidation state,[3e,14a] whereas only a couple of Ni(I)−carbyl molecules have been reported with bidentate ligands.[16] We reasoned that the large bite-angle of Xantphos would help stabilize Ni(I) complexes. After assessing the effect of substituents on Xantphos, we found that *t*Bu-Xantphos stabilizes Ni complexes better than Ph- and *i*Pr-Xantphos, possibly due to the greater steric protection. Our synthesis started with the preparation of (*t*Bu-Xantphos)$NiBr_2$, **1**, by coordination of *t*Bu-Xantphos to $Ni(DME)Br_2$ (Scheme 3).

Scheme 3. Syntheses of (*t*Bu-Xantphos)Ni Complexes

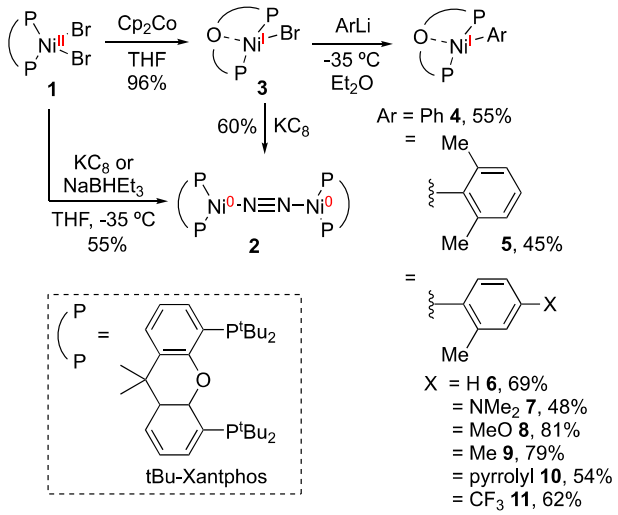

Reduction of **1** with KC_8 or $NaBHEt_3$ afforded (*t*Bu-Xantphos)Ni(N_2), **2**. The X-ray crystal structure of **2** shows that N_2 is bridging between two Ni centers, and the N≡N distance is 1.144(3) Å, only slightly elongated from that of free N_2 (1.098 Å) (Figure 1A). The use of Cp_2Co as the reductant gave (*t*Bu-Xantphos)NiBr, **3**, in 96% yield, which could be further reduced to **2** by KC_8. The X-ray structure of **3** shows a distorted tetrahedral geometry and a relatively long distance between the O atom of *t*Bu-Xantphos and Ni (2.434 Å), indicating a secondary O−Ni interaction (Figure 1B). Phenylation of **3** with phenyllithium at −35 °C generated (*t*Bu-Xantphos)NiPh **4** in 55% yield. X-ray crystallography established a secondary interaction between the O atom of *t*Bu-Xantphos and Ni (2.518 Å) and a distorted tetrahedral geometry (Figure 1C). Broken-symmetry DFT calculations using the ORCA package revealed that the unpaired electron density is concentrated on Ni with a small portion delocalized

DOI: 10.1021/jacs.8b13499
J. Am. Chem. Soc. XXXX, XXX, XXX−XXX

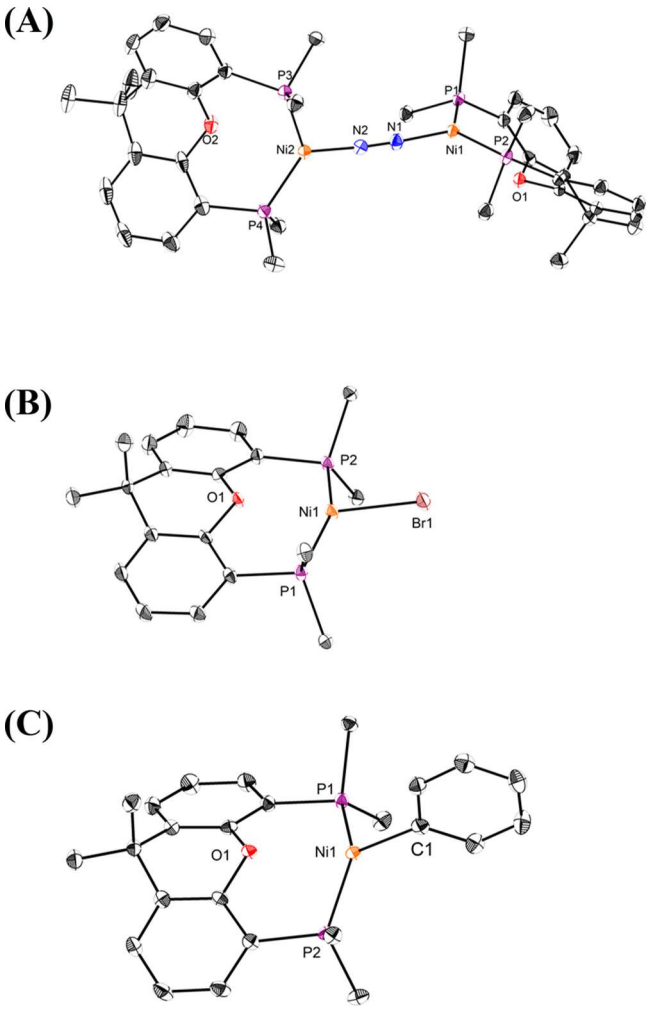

Figure 1. X-ray structures of **2** (A), **3** (B), and **4** (C) at 50% probability thermal ellipsoids. Hydrogen atoms are omitted and *t*-Bu groups are truncated for clarity. Selected bond lengths (Å) for **2**: N(1)≡N(2) = 1.144(3), Ni(1)···O(1) = 2.518. Selected bond length (Å) for **3**: Ni(1)···O(1) = 2.434. Selected bond lengths (Å) for **4**: Ni(1)−C(1) = 1.9795(14), Ni(1)···O(1) = 2.518.

to the Ar group (Figure 2).[17] Arylation of **3** with a variety of aryllithium reagents gave a series of (*t*Bu-Xantphos)NiAr complexes **5**−**11**. The analogous paramagnetic ^{1}H NMR spectra of **5**−**11**, compared to that of **4**, suggest that these compounds have similar electronic structures.

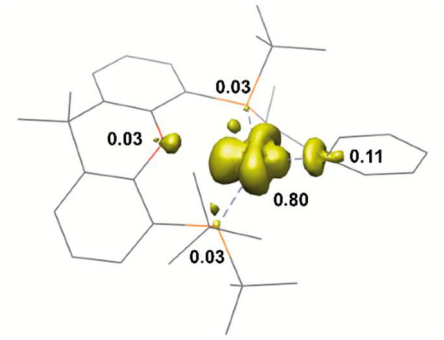

Figure 2. Spin-density plot of **4**.

Ni(0)- and Ni(I)-Mediated Alkyl and Aryl Halide Activation. The isolation of the well-defined (*t*Bu-Xantphos)-Ni(N_2), **2**, and (*t*Bu-Xantphos)Ni−Ar complexes, **4**−**11**, allowed us to carry out a study on their reactivity toward activating alkyl and aryl halides. In C_6D_6, addition of 1 equiv of bromobenzene or chlorobenzene to **2** led to the immediate formation of the corresponding (*t*Bu-Xantphos)Ni−bromide, **3**, or chloride, **13**, respectively, with concomitant formation of biphenyl in high yields (Scheme 4). When (bromomethyl)-cyclopropane **12** was added to **2**, the reaction rapidly formed (*t*Bu-Xantphos), **3**, and 1,7-octadiene in 91% yield.

Scheme 4. Ni(0) Complex 2-Mediated Activation of Alkyl and Aryl Halides

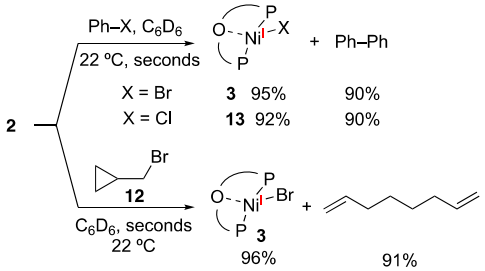

Subsequently, we examined the reactivity of the Ni(I) complexes. (*t*Bu-Xantphos)Ni−Br, **3**, does not react with PhBr, PhI, or **12**. Next we probed the reactivity of (*t*Bu-Xantphos)Ni−*o*-Tol, **6**, toward aryl and alkyl halides (Scheme 5). When 1 equiv of bromobenzene was introduced into a

Scheme 5. Ni(I) Complex 6-Mediated Activation of Alkyl and Aryl Halides

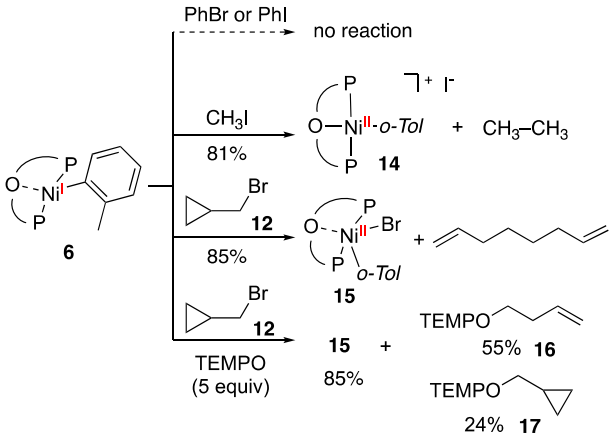

solution of **6** in C_6D_6, no reaction took place after 48 h. Heating the reaction resulted in decomposition of **6**. Addition of CH_3I to **6**, in contrast, led to the formation of the corresponding Ni(II) iodide, **14**, and ethane. Activation of **12** also took place when it was treated with **6** to form Ni(II) bromide, **15**, and 1,7-octadiene in high yields. While the iodide of complex **14** is dissociated from the Ni center to give a square planar geometry, as determined by X-ray crystallography (Figure S20), the bromide from complex **15** is bound to Ni to give a distorted trigonal bipyramidal geometry. When **15** was dissolved in a polar solvent, such as acetone, the bromide dissociated from the Ni center to generate the square planar ionic complex. The reaction rate of **6** with **12** is substantially

DOI: 10.1021/jacs.8b13499
J. Am. Chem. Soc. XXXX, XXX, XXX−XXX

slower than that of **2** with **12**. In situ NMR spectroscopy allowed us to monitor the reaction time course (Figure 3), as

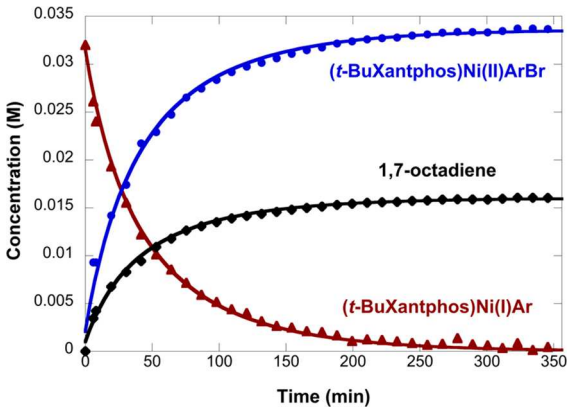

Figure 3. Kinetic profile of (*t*Bu-Xantphos)Ni-*o*-Tol **6**-mediated ring-opening dimerization of cyclopropylmethy bromide **12**. Reaction conditions: $[\mathbf{6}]_0$ = 10 mM, $[\mathbf{12}]_0$ = 12 mM, C_6D_6 = 0.65 mL, 25 °C. Internal standard = mesitylene.

the paramagnetic resonances of **6** could be readily integrated (Figure S37). The time course fits into a second-order kinetic model using COPASI software to give a second-order rate constant (k) of 0.011 M^{-1} s^{-1}.[18] When 5 equiv of TEMPO were included in the reaction of **6** with **12**, the reaction generated a mixture of **16** and **17** as the organic products.

Steric Effects on Ni(I)-Mediated Alkyl Bromide Activation. The clean kinetic profile of (*t*Bu-Xantphos)Ni-*o*-Tol (**6**)-mediated alkyl bromide activation and the formation of the resulting (*t*Bu-Xantphos)Ni(II)(*o*-Tol)(Br), **15**, as a well-defined molecule provided us a special opportunity to elucidate the mechanism of this single-electron oxidative activation process. We initiated our study by investigating the steric and electronic effects of Ni(I) complexes and alkyl bromides on the reaction kinetics. We first compared the activation rates of **12** with a series of increasingly bulky aryl ligands on Ni(I) (Table 1). The reaction of (*t*Bu-Xantphos)-NiPh **4** with **12** proceeded to form 1,7-octadiene with a second-order rate of 0.033 M^{-1} s^{-1} at 25 °C. Compared to that of **4**, the rate of (*t*Bu-Xantphos)Ni-*o*-Tol (**6**)-mediated

Table 1. Steric Effect of the Ar Group on Ni(I)Ar-Mediated Activation of 12[a]

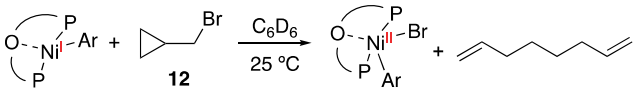

Ar	k x 10^2 ($M^{-1}s^{-1}$)	yield (%)
4	3.3	85
6	1.1	85
5	no reaction	0

[a]Reaction conditions: $[Ni(I)]_0$ = 10 mM, $[\mathbf{12}]_0$ = 20 mM, C_6D_6 = 0.65 mL. Internal standard = mesitylene.

activation of **12** decreased 3-fold and no reaction was observed over 12 h with (*t*Bu-Xantphos)Ni-2,6-dimethylphenyl, **5**.

Our examination of the effect of the alkyl halide was carried out using (*t*Bu-Xantphos)Ni(I) complex **8** as the model molecule (Table 2). Reaction of **8** with 1-bromopropane

Table 2. Steric Effect of Alkyl Bromides on Ni(I)-Mediated Activation[a]

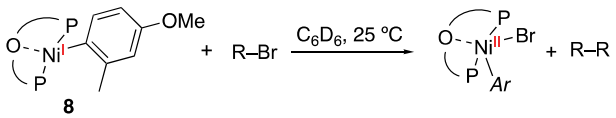

R–	k x 10^3 ($M^{-1}s^{-1}$)	yield (%)
	1.4	73
	6.0	95
	3.8	90

[a]Reaction conditions: $[\mathbf{8}]_0$ = 10 mM, $[R–Br]_0$ = 20 mM, C_6D_6 = 0.65 mL. Internal standard = mesitylene.

proceeded with a second-order rate constant of 1.4×10^{-3} M^{-1} s^{-1} at 25 °C. The reaction with secondary alkyl bromide, 2-bromopropane, was about 4 times faster. The more hindered 4-bromoheptane led to a slightly decreased rate relative to that of 2-bromopropane.

Electronic Effect on Ni(I)-Mediated Alkyl Bromide Activation. The electronic effect of the Ni(I) complexes on the rate of alkyl bromide activation was investigated with a series of *para*- substituted (*t*Bu-Xantphos)NiAr complexes, **6**–**11** (Table 3). The electronic effect of each Ni(I) complex was

Table 3. Electronic Effect on Ni(I)-Mediated Alkyl Bromide Activation

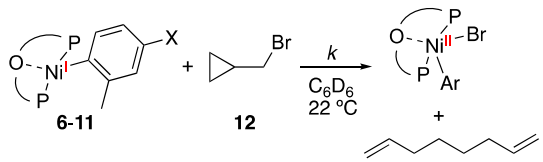

X	σ_p	$E_{1/2}(Ni^{I/II})$ (V vs Fc^+/Fc)	$k \times 10^3$ (M^{-1} s^{-1})
NMe_2 **7**	−0.83	−1.60	27
OMe **8**	−0.27	−1.54	14
Me **9**	−0.17	−1.59	11
H **6**	0	−1.51	11
pyrrolyl **10**	0.37	−1.45	4.2
CF_3 **11**	0.54	−1.37	2.8

parametrized by the electrochemical potentials of the oxidation and reduction in THF solutions. The cyclic voltammetry (CV) of **6** showed quasi-reversible oxidation and reduction waves at −2.70 V and −1.51 V vs Fc/Fc^+ with a scan rate of 250 mV/s, which are assigned to Ni(0)/Ni(I) and Ni(I)/Ni(II) transitions, respectively (Figure 4). With a scan rate of 25 mV/s, the quasi-reversible Ni(0)/Ni(I) transition became irreversible. We attribute this phenomenon to a reversible electron transfer event followed by an irreversible chemical reaction (ErCi).[19] The irreversible chemical reaction rate

DOI: 10.1021/jacs.8b13499
J. Am. Chem. Soc. XXXX, XXX, XXX−XXX

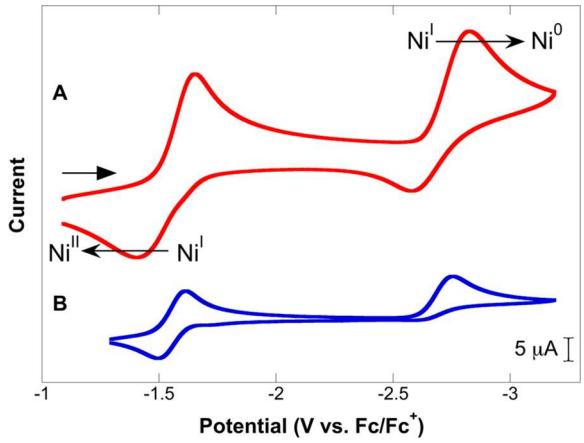

Figure 4. Cyclic voltammetry of **6** in THF. [**6**] = 1 mM, [Bu_4NPF_6] = 0.4 M. (A) scan rate = 250 mV/s; (B) scan rate = 25 mV/s. Internal standard = ferrocene.

varies as the electronic nature of the Ni(I) complex changes (cf. Figures S23−S28). The time-courses of the (*t*Bu-Xantphos)NiAr (**6**−**11**)-mediated single-electron oxidative activations of **12** were monitored by in situ NMR spectroscopy and fit into a second-order kinetic model (Figures S1−S7). The $E_{1/2}$ values for the Ni(I)/Ni(II) transition and the second-order rate constants, *k*, for each of the (*t*Bu-Xantphos)NiAr complexes are summarized in Table 3.

The second-order rate constants, *k*, for the oxidative addition and dimerization of **12** with various (*t*Bu-Xantphos)-NiAr complexes show a linear-free-energy relationship with the Hammett parameters to give a slope (ρ) of −0.72 (Figure 5).

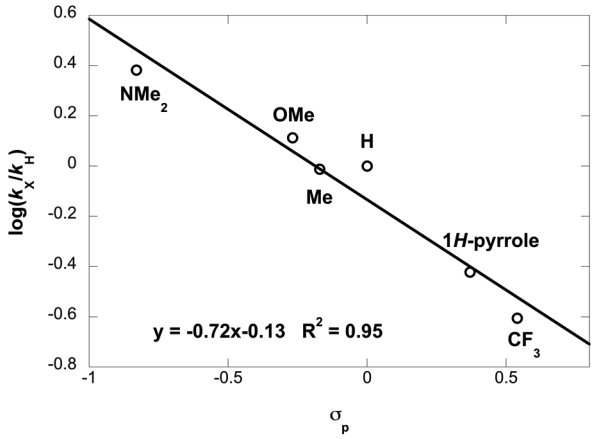

Figure 5. Hammett correlation of the reaction rates of **12** dimerization mediated by complexes **6**−**11**.

The $\Delta G^{\ddagger}$ of each reaction was calculated with *k* using the Eyring equation. The ΔG^0 of each reaction was estimated with the $E_{1/2}$(Ni(I)/Ni(II)) and the Nernst equation. The $\Delta G^{\ddagger}$ varied linearly as a function of ΔG^0, with R^2 of 0.86 and a slope of 0.22 (Figure 6).

Solvent Effect. The effect of solvent on the rate of **8**-mediated activation of isopropyl bromide was investigated with four solvents (Table 4). Monitoring the reactions in pentane-d_{12}, benzene-d_6, DME-d_{12} (dimethoxyethane), and acetone-d_6 revealed similar rates despite the different dielectric constants of the solvents. The reduced rates in polar solvents could be attributed to their coordination to Ni, hindering the approach

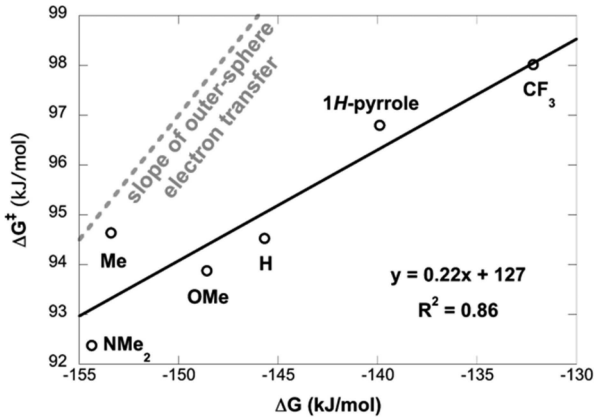

Figure 6. Correlation of the activation energy $\Delta G^{\ddagger}$ (kJ/mol) versus ΔG^0 (kJ/mol).

Table 4. Solvent Effect of 8-Mediated Isopropyl Bromide Activation

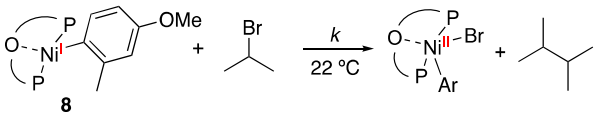

solvent	dielectric constant	$k \times 10^3$ (M^{-1} s^{-1})	yield
pentane-d_{12}	1.8	5.3	80
benzene-d_6	2.3	6.0	95
1,2-DME-d_{10}	7.2	1.8	88
THF-d_6	7.5	0.17	85
acetone-d_6	21	4.3	84

of the alkyl bromides. The rate in THF-d_6 decreased dramatically, and a black precipitate was formed from the reaction. We attribute this outlier to a side pathway triggered by the coordination of THF to **8**. Our attempts to examine the reaction in other polar solvents, including CH_2Cl_2, were complicated by the decomposition of complex **8** in halogenated solvents.

DFT Calculations. Computational studies were performed and compared with the experimental data. We evaluated the four possible pathways (Scheme 2) for the single-electron oxidative activation of EtBr by (*t*Bu-Xantphos)Ni(Ph), **4**, using spin-unrestricted formalism of DFT calculations with the B3LYP functional and the LANL2DZ basis/pseudopotential for the nickel centers and 6-31G(d) for the main-group elements, phosphorus, and bromine. The Gibbs free energy change (ΔG) of −15.6 kcal/mol suggests that the single-electron oxidative activation is exergonic. Optimization for the oxidative addition pathway converged to an S_N2-type mechanism with an activation energy of 17.0 kcal/mol (Figure S57). The outer-sphere electron transfer mechanism was modeled using the Marcus−Hush theory and resulted in a high barrier of 82.8 kcal/mol, suggesting an unfavorable pathway. Evaluation of the inner-sphere electron transfer pathway failed to locate a stable encounter intermediate between **4** and EtBr. Calculations for the halogen-abstraction pathway converged to a concerted transition state **18** with an activation energy of 9.91 kcal/mol (Figure 7A). The geometry of the Ni center in **18** is distorted to a square pyramidal geometry with the phenyl group lifted as the bromide approaches Ni, giving a nearly linear geometry for the C(Ph)−Ni−Br−CH_2CH_3 atoms with a Ni−Br−Et angle of 169°. The spin density plot of **18** shows

DOI: 10.1021/jacs.8b13499
J. Am. Chem. Soc. XXXX, XXX, XXX−XXX

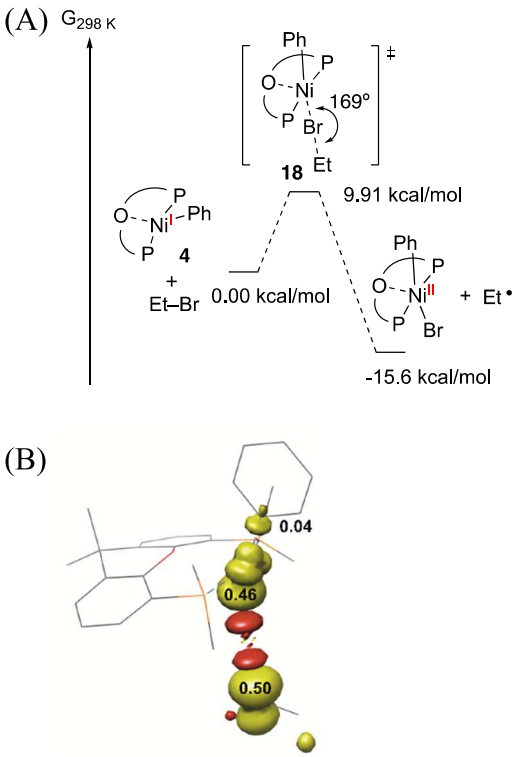

Figure 7. (A) Reaction coordinate for single-electron oxidative activation of EtBr by **4** via concerted halogen-abstraction. Relative Gibbs free energy values were calculated with DFT B3LYP/LANL2DZ/6-31G(d). (B) Spin-density plot of transition state **18**.

that the unpaired electron density is distributed on Ni and CH_2CH_3 (Figure 7B). Within the context of the halogen-abstraction mechanism, we examined the steric effect of the electrophile on the rate of single-electron oxidative activation. When *i*PrBr was used instead of EtBr, the ΔG of the reaction decreased to −16.3 kcal/mol, while the activation energy decreased to 8.53 kcal/mol. Finally, in order to unravel the lack of reactivity of Ni(I) with aryl halides, we calculated the ΔG for phenyl radical generation from PhBr with (*t*Bu-Xantphos)-Ni(Ph) **4**. The ΔG of 1.15 kcal/mol suggests that the activation of sp^2 electrophiles is slightly uphill.

Catalytic Reactivity. While the majority of Ni-catalyzed cross-coupling reactions utilize nitrogen-based ligands, phosphine ligands, such as Xantphos, are competent in a number of cross-coupling reactions.[20] We explored the catalytic relevance of Xantphos ligands to the cross-coupling of alkyl halides. Kumada coupling of benzyl bromide **19** with PhMgBr benefited from the use of a Ph-Xantphos ligand to afford the cross-coupling product **20** in 60% yield, whereas the reaction without a ligand gave **20** in 24% yield (Scheme 6A). Use of the bulkier *t*Bu-Xantphos afforded **21** in 30% yield, suggesting activation of **19** but unsuccessful cross-coupling. Unactivated neopentyl iodide underwent cross-coupling with PhMgBr to give **23** in 83% yield, whereas the reaction with no ligand afforded **23** in 5% yield. Cross-electrophile coupling of **19** with PhI proceeded to generate the desired cross-coupling product **20** in 20% yield with considerable homocoupling byproducts (Scheme 6C). These observations clearly reveal a strong ligand effect on the reactivity and selectivity of the reaction.

Scheme 6. (Xantphos)Ni-Catalyzed Cross-Coupling Reactions

(A) Kumada Coupling of benzyl bromide

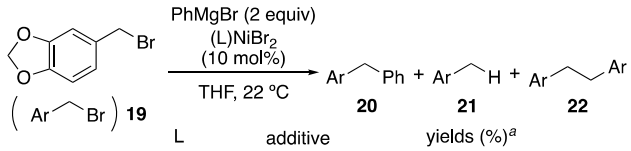

L	additive	yields (%)[a]		
none	$ZnCl_2$	24	0	0
*t*Bu-xantphos	none	trace	30	0
Ph-xantphos	none	38	0	30
Ph-xantphos	**$ZnCl_2$**	**60**	**0**	**15**

[a] Yields determined by ^{1}H NMR with mesitylene as the internal standard.

(B) Kumada Coupling of unactivated alkyl iodide

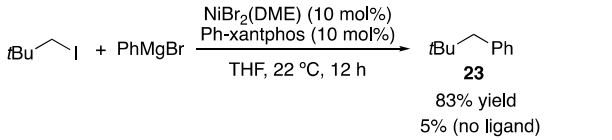

(C) Cross-electrophile coupling

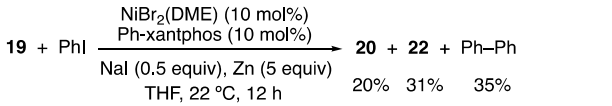

DISCUSSION

The Ni(0) complex (*t*Bu-Xantphos)Ni(N_2) **2** undergoes facile single-electron oxidative activation of aryl and alkyl bromides to form (*t*Bu-Xantphos)NiBr, **3** (Scheme 4). This observation is reminiscent of previous studies on $(PEt_3)_4Ni(0)$.[9] In contrast, Ni(I) complex (*t*Bu-Xantphos)Ni−*o*-Tol, **6**, selectively activates alkyl halides but is inactive toward aryl halides (Scheme 5). We attribute the lack of reactivity with aryl bromides to the instability of aryl radicals, which results in a positive ΔG for the reaction, as determined by DFT calculations. This selective activation of alkyl bromides activation over aryl bromides has important implications in controlling selectivity in cross-electrophile coupling reactions, when both sp^2 and sp^3 electrophiles are present.[1h] The reaction of (*t*Bu-Xantphos)Ni−*o*-Tol **6** with radical clock **12** forms 1,7-octadiene, indicating a radical-mediated ring-opening that precedes the dimerization of the homoallylic radical (Scheme 5). Such radical dimerizations have been extensively observed in catalytic reactions proceeding through radical intermediates.[21] This assignment is supported by the trapping experiment of the cyclopropylmethyl radical with TEMPO to form **16** and **17**. The ratio of **16** to **17** is dependent on the relative rates of cyclopropylmethyl radical ring-opening and trapping by TEMPO.[22]

Four different mechanisms were postulated for the activation of alkyl halides by Ni(I) complexes (Scheme 2), and the results described above provide evidence to distinguish among these possibilities. The slower rate with primary alkyl bromides relative to secondary alkyl bromides (Table 2) rules out the oxidative addition pathway (Scheme 2, *Pathway 1*). This interpretation is consistent with DFT calculations, which show an activation energy of 17.0 kcal/mol for the S_N2 type oxidative addition, substantially higher than that of the halogen abstraction pathway (9.91 kcal/mol). The faster rate of secondary bromide activation, relative to primary bromide

DOI: 10.1021/jacs.8b13499
J. Am. Chem. Soc. XXXX, XXX, XXX−XXX

activation, is reproduced by DFT calculations on the halogen-atom-abstraction pathway and can be attributed to the formation of a more stable secondary radical which has a higher driving force compared to the formation of a primary radical.

The steric effect of aryl groups on Ni and the slope of the linear correlation of $\Delta G^{\ddagger}$ with ΔG^{0}, according to Marcus theory, provides evidence against an outer-sphere electron transfer pathway (Scheme 2, *Pathway 2*). Increased steric hindrance of the Ni complexes significantly reduced the reaction rate (Table 1), whereas outer-sphere electron transfer rates are unlikely to be subject to steric effects.[23] According to Marcus theory,[24] the activation barrier ($\Delta G^{\ddagger}$ of electron transfer would exhibit a linear-free-energy relationship with ΔG^{0} and a slope of 0.5 (eq 1).[25]

$$\Delta G^{\ddagger} = 0.5\Delta G^{0} + \text{constant} \quad (1)$$

The observed slope of 0.22 for the correlation of $\Delta G^{\ddagger}$ to ΔG^{0} significantly deviates from 0.5 (Figure 6), which is inconsistent with the outer-sphere electron transfer pathway. Corroborating this analysis, DFT calculations on the outer-sphere electron transfer pathway returned a very high activation energy of 82.8 kcal/mol.

The difference between the inner-sphere electron transfer (Scheme 2, *Pathway 3*) and the concerted halogen-atom-abstraction pathways (Scheme 2, *Pathway 4*) mainly rests on whether a caged ionic pair is formed as an intermediate. Polar solvents are expected to accelerate the rates of reactions going through an ionic intermediate.[9] In this Ni(I)-mediated single-electron oxidative activation, DME and acetone gave slightly slower rates than those in pentane and benzene (Table 4). We attribute the reduced rates with polar solvents to their coordination to Ni, which hinders the approach of the alkyl bromides. This solvent effect is inconsistent with the inner-sphere electron transfer pathway.

Halogen-atom-abstraction is fully supported by experimental and computational data. The high susceptibility of the rate to the steric effect of the Ni complex (Table 1) indicates association of Ni with the alkyl bromide in the rate-determining step. Such a steric effect is corroborated by the faster rate for 2-bromopropane relative to 4-bromoheptane (Table 2). The encounter of the Ni(I) with the alkyl bromide could be viewed as nucleophilic donation of electron density from Ni(I) to the σ^{*} orbital of the C−Br bond.[26] TS **18** is stabilized by delocalizing electrons among three atoms, Ni, Br, and CH_2CH_3, and forming a three-center-three-electron bond:

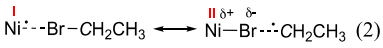

(2)

The nearly linear geometry of **18**, with a Ni−Br−Et angle of 169°, is reminiscent of TS **24** identified for (terpy)NiMe-mediated activation of iodopropane.[13a] In contrast, halogen-abstraction by (py)Ni(Ph) was calculated to have a bent TS **25**.[3h] The activation barriers for **24** and **25** were determined to be 18 and 7.3 kcal/mol, respectively. The barrier of 9.91 kcal/mol for **18** is in between of the two systems. The *trans*-geometry of the aryl group on Ni to the incoming bromide in TS **18** is expected to enhance the electronic effect on the rate. The Hammett correlation of the rates with *para*-substituted Ni−aryl complexes indicates a buildup of partial positive charge on Ni in transition state (TS) **18**. A similar electronic effect has been proposed for **24**.[13a] The slope of −0.72 is similar to previous reactions going through a concerted mechanism.[27] The Marcus dependence of $\Delta G^{\ddagger}$ as a function of ΔG^{0} shows an unusually shallow slope of 0.22. A comparable slope has been reported in a C−H oxidation reaction, going through concerted PCET (proton-coupled-electron-transfer).[28] While the origin of the moderate slope is unclear in either system, studies to explain it are underway.

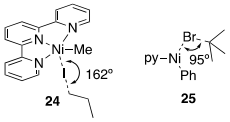

SUMMARY

We prepared a series of (*t*Bu-Xantphos)Ni(I)−Ar complexes that selectively activate alkyl halides over aryl halides via single-electron oxidative activation to eject alkyl radicals. Kinetic studies on the steric, electronic, and solvent effects, in combination with DFT calculations, reveal that the single-electron oxidative activation of alkyl halides proceeds via a concerted halogen-atom-abstraction mechanism, in contrast with the previous proposal of outer-sphere electron transfer for Ni(0)-mediated aryl halide activation[9] and consistent with recent DFT calculations on Ni(I) systems.[13] Corroborated by the stoichiometric study, Xantphos is shown to promote catalytic cross-coupling of unactivated alkyl halides. The selective reactivity of (Xantphos)Ni(I) toward alkyl halides, relative to aryl halides, and the elucidation of the mechanism, as a case study, provide insight into the mechanism of Ni-catalyzed cross-coupling reactions. However, whether the mechanism could be generalized remains to be seen, and the insight obtained here should be cautiously applied to other systems.

ASSOCIATED CONTENT

Supporting Information

The Supporting Information is available free of charge on the ACS Publications website at DOI: 10.1021/jacs.8b13499.

Experimental procedures, additional figures, details of DFT calculations, NMR spectra (PDF)

Crystallographic data for (*t*-BuXantphos)Ni(II) 4-pyrrolylphenyl bromide (CIF), (*t*-BuXantphos)Ni 2-methyl-4-trifluoromethylphenyl (**11**, CIF), (*t*-BuXantphos)NiPh (**4**, CIF), (*t*-BuXantphos)Ni(II) phenyl bromide (CIF), (*t*-BuXantphos)Ni(II)Br_2 (**1**, CIF), (*t*-BuXantphos)NiBr (**3**, CIF), (*t*-BuXantphos)Ni o-tolyl iodide (**14**, CIF), (*t*-BuXantphos)Ni o-tolyl (CIF), [(*t*-BuXantphos)Ni(0)]$_2N_2$ (**2**, CIF)

AUTHOR INFORMATION

Corresponding Author

*diao@nyu.edu

ORCID

Chunhua Hu: 0000-0002-8172-2202

Tianning Diao: 0000-0003-3916-8372

Notes

The authors declare no competing financial interest.

ACKNOWLEDGMENTS

This work was supported by the National Science Foundation under award number DMR-1420073 and ACS-Petroleum Research Foundation (56568-DNI3). J.D. is supported by the Margaret and Herman Sokol Fellowship and the Ted Keusseff

Fellowship. T.D. is a recipient of the Alfred P. Sloan Research Fellowship (FG-2018-10354).

■ REFERENCES

(1) For reviews, see (a) Netherton, M. R.; Fu, G. C. Nickel-Catalyzed Cross-Couplings of Unactivated Alkyl Halides and Pseudohalides with Organometallic Compounds. *Adv. Synth. Catal.* **2004**, *346*, 1525. (b) Tamaru, Y. *Modern Organonickel Chemistry*; Wiley-VCH: Weinheim, 2005. (c) Rosen, B. M.; Quasdorf, K. W.; Wilson, D. A.; Zhang, N.; Resmerita, A.-M.; Garg, N. K.; Percec, V. Nickel-Catalyzed Cross-Couplings Involving Carbon−Oxygen Bonds. *Chem. Rev.* **2011**, *111*, 1346. (d) Jahn, U. In *Radicals in Synthesis III*; Heinrich, M., Gansäuer, A., Eds.; Springer: Berlin Heidelberg, 2012; Vol. *320*, p 323. (e) Tasker, S. Z.; Standley, E. A.; Jamison, T. F. Recent Advances in Homogeneous Nickel Catalysis. *Nature* **2014**, *509*, 299. (f) Su, B.; Cao, Z.-C.; Shi, Z.-J. Exploration of Earth-Abundant Transition Metals (Fe, Co, and Ni) as Catalysts in Unreactive Chemical Bond Activations. *Acc. Chem. Res.* **2015**, *48*, 886. (g) Standley, E. A.; Tasker, S. Z.; Jensen, K. L.; Jamison, T. F. Nickel Catalysis: Synergy between Method Development and Total Synthesis. *Acc. Chem. Res.* **2015**, *48*, 1503. (h) Weix, D. J. Methods and Mechanisms for Cross-Electrophile Coupling of Csp^2 Halides with Alkyl Electrophiles. *Acc. Chem. Res.* **2015**, *48*, 1767. (i) Choi, J.; Fu, G. C. Transition Metal-Catalyzed Alkyl-Alkyl Bond Formation: Another Dimension in Cross-Coupling Chemistry. *Science* **2017**, *356*, eaaf7230. (j) Fu, G. C. Transition-Metal Catalysis of Nucleophilic Substitution Reactions: A Radical Alternative to S_N1 and S_N2 Processes. *ACS Cent. Sci.* **2017**, *3*, 692.

(2) (a) Hegedus, L. S.; Miller, L. L. Reaction of π-Allylnickel Bromide Complexes With Organic Halides. Stereochemistry and Mechanism. *J. Am. Chem. Soc.* **1975**, *97*, 459. (b) Tsou, T. T.; Kochi, J. K. Mechanism of Biaryl Synthesis With Nickel Complexes. *J. Am. Chem. Soc.* **1979**, *101*, 7547. (d) Hegedus, L. S.; Thompson, D. H. P. The Reactions of Organic Halides With (π-Allyl)nickel Halide Complexes: a Mechanistic Study. *J. Am. Chem. Soc.* **1985**, *107*, 5663. (e) Yamamoto, T.; Wakabayashi, S.; Osakada, K. Mechanism of C−C Coupling Reactions of Aromatic Halides, Promoted by $Ni(COD)_2$ in the Presence of 2,2'-bypyridine and PPh_3 to Give Biaryls. *J. Organomet. Chem.* **1992**, *428*, 223.

(3) (a) Jones, G. D.; Martin, J. L.; McFarland, C.; Allen, O. R.; Hall, R. E.; Haley, A. D.; Brandon, R. J.; Konovalova, T.; Desrochers, P. J.; Pulay, P.; Vicic, D. A. Ligand Redox Effects in the Synthesis, Electronic Structure, and Reactivity of an Alkyl−Alkyl Cross-Coupling Catalyst. *J. Am. Chem. Soc.* **2006**, *128*, 13175. (b) Cornella, J.; Gómez-Bengoa, E.; Martin, R. Combined Experimental and Theoretical Study on the Reductive Cleavage of Inert C−O Bonds with Silanes: Ruling out a Classical Ni(0)/Ni(II) Catalytic Couple and Evidence for Ni(I) Intermediates. *J. Am. Chem. Soc.* **2013**, *135*, 1997. (c) Breitenfeld, J.; Ruiz, J.; Wodrich, M. D.; Hu, X. Bimetallic Oxidative Addition Involving Radical Intermediates in Nickel-Catalyzed Alkyl−Alkyl Kumada Coupling Reactions. *J. Am. Chem. Soc.* **2013**, *135*, 12004. (d) Biswas, S.; Weix, D. J. Mechanism and Selectivity in Nickel-Catalyzed Cross-Electrophile Coupling of Aryl Halides with Alkyl Halides. *J. Am. Chem. Soc.* **2013**, *135*, 16192. (e) Schley, N. D.; Fu, G. C. Nickel-Catalyzed Negishi Arylations of Propargylic Bromides: A Mechanistic Investigation. *J. Am. Chem. Soc.* **2014**, *136*, 16588. (f) Mohadjer Beromi, M.; Nova, A.; Balcells, D.; Brasacchio, A. M.; Brudvig, G. W.; Guard, L. M.; Hazari, N.; Vinyard, D. J. Mechanistic Study of an Improved Ni Precatalyst for Suzuki−Miyaura Reactions of Aryl Sulfamates: Understanding the Role of Ni(I) Species. *J. Am. Chem. Soc.* **2017**, *139*, 922. (g) Manzoor, A.; Wienefeld, P.; Baird, M. C.; Budzelaar, P. H. M. Catalysis of Cross-Coupling and Homocoupling Reactions of Aryl Halides Utilizing Ni(0), Ni(I), and Ni(II) Precursors; Ni(0) Compounds as the Probable Catalytic Species but Ni(I) Compounds as Intermediates and Products. *Organometallics* **2017**, *36*, 3508. (h) Wang, X.; Ma, G.; Peng, Y.; Pitsch, C. E.; Moll, B. J.; Ly, T. D.; Wang, X.; Gong, H. Ni-Catalyzed Reductive Coupling of Electron-Rich Aryl Iodides with Tertiary Alkyl Halides. *J. Am. Chem. Soc.* **2018**, *140*, 14490. (i) Shevick, S. L.; Obradors, C.; Shenvi, R. A. Mechanistic Interrogation of Co/Ni-Dual Catalyzed Hydroarylation. *J. Am. Chem. Soc.* **2018**, *140*, 12056.

(4) For a recent review, see Hu, X. Nickel-Catalyzed Cross Coupling of Non-Activated Alkyl Halides: A Mechanistic Perspective. *Chem. Sci.* **2011**, *2*, 1867.

(5) (a) Cherney, A. H.; Kadunce, N. T.; Reisman, S. E. Enantioselective and Enantiospecific Transition-Metal-Catalyzed Cross-Coupling Reactions of Organometallic Reagents To Construct C−C Bonds. *Chem. Rev.* **2015**, *115*, 9587. (b) Lucas, E. L.; Jarvo, E. R. Stereospecific and Stereoconvergent Cross-Couplings Between Alkyl Electrophiles. *Nature Reviews Chemistry* **2017**, *1*, 0065.

(6) (a) Tellis, J. C.; Primer, D. N.; Molander, G. A. Single-Electron Transmetalation in Organoboron Cross-Coupling by Photoredox/Nickel Dual Catalysis. *Science* **2014**, *345*, 433. (b) Zuo, Z.; Ahneman, D. T.; Chu, L.; Terrett, J. A.; Doyle, A. G.; MacMillan, D. W. C. Merging Photoredox with Nickel Catalysis: Coupling of α-Carboxyl sp^3-Carbons with Aryl Halides. *Science* **2014**, *345*, 437.

(7) Lipschutz, M. I.; Yang, X.; Chatterjee, R.; Tilley, T. D. A Structurally Rigid Bis(amido) Ligand Framework in Low-Coordinate Ni(I), Ni(II), and Ni(III) Analogues Provides Access to a Ni(III) Methyl Complex via Oxidative Addition. *J. Am. Chem. Soc.* **2013**, *135*, 15298.

(8) (a) Stolzenberg, A. M.; Stershic, M. T. Reactions of the Nickel(I) Octaethylisobacteriochlorin Anion with Alkyl Halides. *J. Am. Chem. Soc.* **1988**, *110*, 5397. (b) Lahiri, G. K.; Stolzenberg, A. M. F430 Model Chemistry. Evidence for Alkyl- and Hydrido-Nickel Intermediates in the Reactions of the Nickel(I) Octaethylisobacteriochlorin Anion. *Inorg. Chem.* **1993**, *32*, 4409. (c) Gutierrez, O.; Tellis, J. C.; Primer, D. N.; Molander, G. A.; Kozlowski, M. C. Nickel-Catalyzed Cross-Coupling of Photoredox-Generated Radicals: Uncovering a General Manifold for Stereoconvergence in Nickel-Catalyzed Cross-Couplings. *J. Am. Chem. Soc.* **2015**, *137*, 4896.

(9) Tsou, T. T.; Kochi, J. K. Mechanism of Oxidative Addition. Reaction of Nickel(0) Complexes with Aromatic Halides. *J. Am. Chem. Soc.* **1979**, *101*, 6319.

(10) Zhang, K.; Conda-Sheridan, M. R.; Cooke, S.; Louie, J. N-Heterocyclic Carbene Bound Nickel(I) Complexes and Their Roles in Catalysis. *Organometallics* **2011**, *30*, 2546.

(11) Bakac, A.; Espenson, J. H. Kinetics and mechanism of the alkylnickel formation in one-electron reductions of alkyl halides and hydroperoxides by a macrocyclic nickel(I) complex. *J. Am. Chem. Soc.* **1986**, *108*, 713.

(12) (a) Funes-Ardoiz, I.; Nelson, D. J.; Maseras, F. Halide Abstraction Competes with Oxidative Addition in the Reactions of Aryl Halides with $[Ni(PMe_nPh_{(3-n)})_4]$. *Chem. - Eur. J.* **2017**, *23*, 16728. (b) Kehoe, R.; Mahadevan, M.; Manzoor, A.; McMurray, G.; Wienefeld, P.; Baird, M. C.; Budzelaar, P. H. M. Reactions of the Ni(0) Compound $Ni(PPh_3)_4$ with Unactivated Alkyl Halides: Oxidative Addition Reactions Involving Radical Processes and Nickel(I) Intermediates. *Organometallics* **2018**, *37*, 2450.

(13) (a) Lin, X.; Phillips, D. L. Density Functional Theory Studies of Negishi Alkyl−Alkyl Cross-Coupling Reactions Catalyzed by a Methylterpyridyl-Ni(I) Complex. *J. Org. Chem.* **2008**, *73*, 3680. (b) Some experimental data are also provided in this study: Yoo, C.; Ajitha, M. J.; Jung, Y.; Lee, Y. Mechanistic Study on C−C Bond Formation of a Nickel(I) Monocarbonyl Species with Alkyl Iodides: Experimental and Computational Investigations. *Organometallics* **2015**, *34*, 4305. (c) Lin, X.; Sun, J.; Xi, Y.; Lin, D. How Racemic Secondary Alkyl Electrophiles Proceed to Enantioselective Products in Negishi Cross-Coupling Reactions. *Organometallics* **2011**, *30*, 3284−3292.

(14) (a) Anderson, T. J.; Jones, G. D.; Vicic, D. A. Evidence for a Ni^I Active Species in the Catalytic Cross-Coupling of Alkyl Electrophiles. *J. Am. Chem. Soc.* **2004**, *126*, 8100. (b) Laskowski, C. A.; Bungum, D. J.; Baldwin, S. M.; Del Ciello, S. A.; Iluc, V. M.; Hillhouse, G. L. Synthesis and Reactivity of Two-Coordinate Ni(I) Alkyl and Aryl Complexes. *J. Am. Chem. Soc.* **2013**, *135*, 18272.

(15) (a) Lin, C.-Y.; Power, P. P. Complexes of Ni(I): A "Rare" Oxidation State of Growing Importance. *Chem. Soc. Rev.* **2017**, *46*,

DOI: 10.1021/jacs.8b13499
J. Am. Chem. Soc. XXXX, XXX, XXX−XXX

5347. (b) Zimmermann, P.; Limberg, C. Activation of Small Molecules at Nickel(I) Moieties. *J. Am. Chem. Soc.* **2017**, *139*, 4233.

(16) (a) Kitiachvili, K. D.; Mindiola, D. J.; Hillhouse, G. L. Preparation of Stable Alkyl Complexes of Ni(I) and Their One-Electron Oxidation to Ni(II) Complex Cations. *J. Am. Chem. Soc.* **2004**, *126*, 10554. (b) Kuang, Y.; Anthony, D.; Katigbak, J.; Marrucci, F.; Humagain, S.; Diao, T. Ni(I)-Catalyzed Reductive Cyclization of 1,6-Dienes: Mechanism-Controlled trans Selectivity. *Chem.* **2017**, *3*, 268. (c) Mohadjer Beromi, M.; Banerjee, G.; Brudvig, G. W.; Hazari, N.; Mercado, B. Q. Nickel(I) Aryl Species: Synthesis, Properties, and Catalytic Activity. *ACS Catal.* **2018**, *8*, 2526.

(17) Neese, F. The ORCA Program System. *Wiley Interdisciplinary Reviews: Computational Molecular Science* **2012**, *2*, 73.

(18) Hoops, S.; Sahle, S.; Gauges, R.; Lee, C.; Pahle, J.; Simus, N.; Singhal, M.; Xu, L.; Mendes, P.; Kummer, U. COPASI—A COmplex PAthway SImulator. *Bioinformatics* **2006**, *22*, 3067.

(19) Elgrishi, N.; Kurtz, D. A.; Dempsey, J. L. Reaction Parameters Influencing Cobalt Hydride Formation Kinetics: Implications for Benchmarking H_2-Evolution Catalysts. *J. Am. Chem. Soc.* **2017**, *139*, 239.

(20) (a) Staudaher, N. D.; Stolley, R. M.; Louie, J. Synthesis, Mechanism of Formation, and Catalytic Activity of Xantphos Nickel π-Complexes. *Chem. Commun.* **2014**, *50*, 15577. (b) Erickson, L. W.; Lucas, E. L.; Tollefson, E. J.; Jarvo, E. R. Nickel-Catalyzed Cross-Electrophile Coupling of Alkyl Fluorides: Stereospecific Synthesis of Vinylcyclopropanes. *J. Am. Chem. Soc.* **2016**, *138*, 14006. (c) Cao, X.; Sha, S.-C.; Li, M.; Kim, B.-S.; Morgan, C.; Huang, R.; Yang, X.; Walsh, P. J. Nickel-Catalyzed Arylation of Heteroaryl-Containing Diarylmethanes: Exceptional Reactivity of the Ni(NIXANTPHOS)-based Catalyst. *Chem. Sci.* **2016**, *7*, 611. (d) Wang, J.; Meng, G.; Xie, K.; Li, L.; Sun, H.; Huang, Z. Mild and Efficient Ni-Catalyzed Biaryl Synthesis with Polyfluoroaryl Magnesium Species: Verification of the Arrest State, Uncovering the Hidden Competitive Second Transmetalation and Ligand-Accelerated Highly Selective Monoarylation. *ACS Catal.* **2017**, *7*, 7421.

(21) (a) Poizot, P.; Jouikov, V.; Simonet, J. Glassy Carbon Modified by a Silver−Palladium Alloy: Cheap and Convenient Cathodes for the Selective Reductive Homocoupling of Alkyl Iodides. *Tetrahedron Lett.* **2009**, *50*, 822. (b) Prinsell, M. R.; Everson, D. A.; Weix, D. J. Nickel-Catalyzed, Sodium Iodide-Promoted Reductive Dimerization of Alkyl Halides, Alkyl Pseudohalides, and Allylic Acetates. *Chem. Commun.* **2010**, *46*, 5743. (c) Manley, D. W.; Walton, J. C. A Clean and Selective Radical Homocoupling Employing Carboxylic Acids with Titania Photoredox Catalysis. *Org. Lett.* **2014**, *16*, 5394.

(22) (a) Bowry, V. W.; Lusztyk, J.; Ingold, K. U. Evidence for Reversible Ring-Opening of the α-Cyclopropylbenzyl Radical. *J. Chem. Soc., Chem. Commun.* **1990**, *0*, 923. (b) Hollis, R.; Hughes, L.; Bowry, V. W.; Ingold, K. U. Calibration of a Fast Benzylic Radical Clock Reaction. *J. Org. Chem.* **1992**, *57*, 4284.

(23) Wong, C. L.; Kochi, J. K. Electron Transfer with Organometals. Steric Effects as Probes for Outer-Sphere and Inner-Sphere Oxidations of Homoleptic Alkylmetals with Iron(III) and Iridate(IV) Complexes. *J. Am. Chem. Soc.* **1979**, *101*, 5593.

(24) Marcus, R. A. On the Theory of Oxidation-Reduction Reactions Involving Electron Transfer. I. *J. Chem. Phys.* **1956**, *24*, 966.

(25) Darcy, J. W.; Koronkiewicz, B.; Parada, G. A.; Mayer, J. M. A Continuum of Proton-Coupled Electron Transfer Reactivity. *Acc. Chem. Res.* **2018**, *51*, 2391.

(26) Danen, W. C.; Saunders, D. G. Halogen Abstraction Reactions. I. Free-Radical Abstraction of Iodine from Substituted Iodobenzenes. *J. Am. Chem. Soc.* **1969**, *91*, 5924.

(27) Lalic, G.; Krinsky, J. L.; Bergman, R. G. Scope and Mechanism of Formal S_N2' Substitution Reactions of a Monomeric Imidozirconium Complex with Allylic Electrophiles. *J. Am. Chem. Soc.* **2008**, *130*, 4459.

(28) Markle, T. F.; Darcy, J. W.; Mayer, J. M. A New Strategy to Efficiently Cleave and Form C−H Bonds Using Proton-Coupled Electron Transfer. *Sci. Adv.* **2018**, *4*.eaat5776

DOI: 10.1021/jacs.8b13499
J. Am. Chem. Soc. XXXX, XXX, XXX−XXX